**Supplementary Information for:**

# Design and characterization of rapid optogenetic circuits for dynamic control in yeast metabolic engineering

Evan M. Zhao[1], Makoto A. Lalwani[1], Robert J. Lovelett[1,2], Sergio A. García-Echauri[1], Shannon M. Hoffman[1], Christopher L. Gonzalez[1], Jared E. Toettcher[3], Ioannis G. Kevrekidis[1,2], & José L. Avalos[1,3,4,*]

1. Department of Chemical and Biological Engineering, Hoyt Laboratory 101, Princeton University, William Street, Princeton, NJ 08544, USA
2. Department of Chemical and Biomolecular Engineering, 221 Maryland Hall, 2400 N. Charles Street, Johns Hopkins University, Baltimore, MD 21218, USA
3. Department of Molecular Biology, 140 Lewis Thomas Laboratory, Washington Road, Princeton, NJ 08544, USA
4. The Andlinger Center for Energy and the Environment, Princeton University, 86 Olden Street, Princeton, NJ 08544, USA

* Correspondence: javalos@princeton.edu

**Supplementary discussion on lactic acid fermentation**

The enhanced kinetics of OptoINVRT7 allows optimal chemical production to occur at higher cell densities, resulting in higher titers. The optimal $\rho_s$ for lactic acid production with OptoINVRT2 (YEZ212C) is 3.5, while the optimal $\rho_s$ with OptoINVRT7 (YEZ212) is 7 (Fig. 4b). Because there are no differences in these strains other than the OptoINVRT circuit they contain, we can conclude that changes in production are solely due to differences in circuit dynamics. Due to its faster light-to-dark kinetics, OptoINVRT7 produces more LDH faster than OptoINVRT2, allowing it to better compete with *PDC1*, even at $\rho_s$ values higher than 3.5, resulting in higher LA production. By having a higher optimal $\rho_s$ and thus operating at a higher cell density throughout the fermentation, OptoINVRT7 produces as much as 53.6 ± 8.4% more LA than OptoINVRT2 at its optimal $\rho_s$ (Fig. 4b). Therefore, enabling high lactic acid production at higher $\rho_s$ compounds higher LDH activity with higher cell density for a significant boost in production.

Furthermore, the rapid induction of LDH afforded by OptoINVRT7 seems to better compensate for the reduced expression of *PDC1* upon switching to dark conditions, compared to OptoINVRT2 (Supplementary Fig. 9c). We observe that for every $\rho_s$, the strain with OptoINVRT2 is unable to reach the same final cell density achieved in full light. In contrast, the final cell densities of fermentations with the strain containing OptoINVRT7 operated at $\rho_s$ of 7.0 or above are much closer to the density achieved in full light (Supplementary Fig. 9c). The activity of LDH involves oxidizing NADH to $NAD^+$ and can thus replace, to some extent, this metabolic role of Pdc1p that is diminished in the dark. Therefore, by allowing strong induction

of LDH at higher cell densities (ρ=7.0-9.5), the strain containing OptoINVRT7 is able to reach almost the same final cell density as in full light (Supplementary Fig. 9c) despite producing less ethanol (Supplementary Fig. 9b) because it produces more LA (Fig. 4b and Supplementary Fig. 9a). This effect of inducing LDH rapidly later in the fermentation, enabled by OptoINVRT7, thus combines higher biomass accumulation with prolonged cell growth in the dark and higher LDH activity for higher LA production.

Another important difference is that OptoINVRT7 is less leaky than OptoINVRT2 when cells are grown under full light (Fig. 1c). The reason is likely the light sensitive degron domain fused to Gal4p, which lowers its basal activity level in the light. This is another advantage of OptoINVRT7 in cases where the product of interest is toxic to the cell and it would be desirable to keep its production repressed during cell growth.

**Supplementary Sequences**

Supplementary Sequence 1 - ODCmut:

TTTCCCCCCGAAGTTGAAGAGCAAGATGACGGGACATTACCTATGTCTTGTGCCCAG
GAATCAGGGATGGATAGACACCCAGCTTCTTGTCCAGAAAGGGCCGCATGTGCTTC
AGCCAGGATAAACGTA

Supplementary Sequence 2 – $P_{GAL1\text{-}M}$:

CGGATTAGAAGCCGCCGAGCGGGTGACAGCCCTCCGAAGGAAGACTCTCCTCCGTG
CGTCCTCGTCTTCACCGGTCGCGTTCCTGAAACGCAGATGTGCCTCGCGCCGCACTG
CTCCGAACAATAAAGATTCTACAATACTAGCTTTTATGGTTATGAAGAGGAAAAATT

GGCAGTAACCTGGTTGGTAAAACCTTCAAATGAACGAATCAAATTAACAACCATAG

GATGATAATGCGATTAGTTTTTTAGCCTTATTTTAGTAGTAATTAATCAGCGAAGCG

ATGATTTTTGATCTATTAACAGATATATAAATGCAAAAACTGCATAACCACTTTAAC

TAATACTTTCAACATTTTCGGTTTGTATTACTTCTTATTCAAATGTAATAAAAGTATC

AACAAAAAATTGTTAATATACCTCTATACTTTAACGTCAAGGAGAAAAAACTATA

Supplementary Sequence 3 – $P_{GAL1\text{-}S}$:

CGGATTAGAAGCCGCCGAGCGGGTGACAGCCCTCCGAAGGAAGACTCTCCTCCGTG

CGTCCTCGTCTTCACCGGTCGCGTTCCTGAAACGCAGATGTGCCTCGCGCCGCACTG

CTCCGAACAATAAAGATTCTACAATACTAGCTTTTATGGTTATGAAGAGGAAAAATT

GGATGATTTTTGATCTATTAACAGATATATAAATGCAAAAACGGATTAGAAGCCGCC

GAGCGGGTGACAGCCCTCCGAAGGAAGACTCTCCTCCGTGCGTCCTCGTCTTCACCG

GTCGCGTTCCTGAAACGCAGATGTGCCTCGCGCCGCACTGCTCCGAACAATAAAGAT

TCTACAATACTAGCTTTTATGGTTATGAAGAGGAAAAATTGGCAGTAACCTGGTTGG

TAAAACCTTCAAATGAACGAATCAAATTAACAACCATAGGATGATAATGCGATTAG

TTTTTTAGCCTTATTTTAGTAGTAATTAATCAGCGAAGCGATGATTTTTGATCTATTA

ACAGATATATAAATGCAAAAACTGCATAACCACTTTAACTAATACTTTCAACATTTT

CGGTTTGTATTACTTCTTATTCAAATGTAATAAAAGTATCAACAAAAAATTGTTAAT

ATACCTCTATACTTTAACGTCAAGGAGAAAAAACTATA

110

111 **Supplementary Table 1.** Plasmids used in study.

| **Plasmid** | **Position 1** | **Position 2** | **Position 3** | **Position 4** | **Position 5** | **Marker** | **Vector type** | **Source** |
|---|---|---|---|---|---|---|---|---|
| pJLA121$^{0301}$ | $P_{PGK1}$_ MCS_$T_{CYC1}$ | EMPTY | EMPTY | EMPTY | EMPTY | *URA3* | 2µ | [1] |
| pYZ12-B | EMPTY | EMPTY | EMPTY | EMPTY | EMPTY | *HIS3*$_{Cg}$ | *HIS3* locus Integration | [2] |
| pYZ23 | EMPTY | EMPTY | EMPTY | EMPTY | EMPTY | Zeocin | δ-sites Integration | [2] |
| EZ-L164 | $P_{GAL1}$_GFP_ $T_{ADH1}$ | EMPTY | EMPTY | EMPTY | EMPTY | *HIS3*$_{Cg}$ | *HIS3* locus Integration | This Study |
| EZ-L260 | $P_{TEF1}$_ VP16-EL222 _$T_{CYC1}$ | $P_{C120}$_*GAL80*_ $T_{ACT1}$ | $P_{GAL1}$_GFP_ $T_{ADH1}$ | $P_{PGK1}$_*GAL4*_T $_{ACT1}$ | $P_{C120}$_*GAL*80_ $T_{ADH1}$ | *HIS3*$_{Cg}$ | *HIS3* locus Integration | This Study |
| EZ-L352 | $P_{C120}$_*PDC1*_T | $P_{GAL1\text{-}M}$_ | EMPTY | EMPTY | EMPTY | Zeocin | δ-sites | This |

| | | | | | | | | |
|---|---|---|---|---|---|---|---|---|
| | $_{ACT1}$ | *ILV2*_ $T_{ADH1}$ | | | | | integration | Study |
| EZ-L353 | $P_{C120}$_*PDC1*_T $_{ACT1}$ | $P_{GAL1-M}$_ *LDH*_ $T_{ADH1}$ | EMPTY | EMPTY | EMPTY | Zeocin | δ-sites integration | This Study |
| EZ-L390 | $P_{PGK1}$_*ILV3*_T $_{CYC1}$ | $P_{TEF1}$_CoxIV_ LlAdhA$^{RE1}$_ $T_{ACT1}$ | $P_{GAL1-M}$_ *ILV2*_$T_{ADH1}$ | $P_{TEF1}$_*ILV5*_$T_{A}$ $_{CT1}$ | $P_{TDH3}$_CoxIV_ *ARO10*_ $T_{ADH1}$ | *URA3* | 2μ | This Study |
| EZ-L400 | $P_{TEF1}$_ VP16-EL222 _$T_{CYC1}$ | $P_{C120}$_*GAL80*_ *CLN2PEST*_T $_{ACT1}$ | $P_{GAL1}$_GFP_ $T_{ADH1}$ | $P_{C120}$_*GAL*80_ *CLN2PEST* _$T_{ACT1}$ | $P_{PGK1}$_*GAL*4_P SD_$T_{ADH1}$ | $HIS3_{Cg}$ | *HIS3* locus Integration | This Study |
| EZ-L417 | $P_{GAL1-S}$_ MCS_$T_{ADH1}$ | EMPTY | EMPTY | EMPTY | EMPTY | *URA3* | 2μ | This Study |
| EZ-L436 | $P_{TEF1}$_ VP16-EL222 _$T_{CYC1}$ | $P_{C120}$_*GAL80*_ *ODCmut*_ $T_{ACT1}$ | $P_{GAL1-S}$_GFP_ $T_{ADH1}$ | $P_{C120}$_*GAL80*_ *ODCmut*_$T_{ACT}$ $_{1}$ | $P_{PGK1}$_*GAL*4_P SD_$T_{ADH1}$ | $HIS3_{Cg}$ | *HIS3* locus Integration | This Study |
| EZ-L437C | $P_{TEF1}$_ | $P_{C120}$_*GAL80*_ | $P_{GAL1}$_GFP_ | $P_{C120}$_*GAL80*_ | $P_{PGK1}$_*GAL*4_P | $HIS3_{Cg}$ | *HIS3* locus Integration | This |

| | | | | | | | | |
|---|---|---|---|---|---|---|---|---|
| | VP16-EL222 _$T_{CYC1}$ | *ODCmut*_ $T_{ACT1}$ | $T_{ADH1}$ | *ODCmut*_ $T_{ACT1}$ | SD_$T_{ADH1}$ | | | Study |
| EZ-L437 | $P_{TEF1}$_ VP16-EL222 _$T_{CYC1}$ | $P_{C120}$_*GAL80*_ *ODCmut*_ $T_{ACT1}$ | $P_{GAL1-M}$_ GFP_$T_{ADH1}$ | $P_{C120}$_*GAL80*_ *ODCmut*_ $T_{ACT1}$ | $P_{PGK1}$_*GAL4*_P SD_$T_{ADH1}$ | $HIS3_{Cg}$ | *HIS3* locus Integration | This Study |
| EZ-L439 | $P_{TEF1}$_VP16-EL222 _$T_{CYC1}$ | $P_{C120}$_*GAL80*_ *ODCmut*_ $T_{ACT1}$ | EMPTY | $P_{PGK1}$_*GAL4*_P SD_$T_{ADH1}$ | $P_{C120}$_*GAL80*_ *ODCmut*_ $T_{ACT1}$ | $HIS3_{Cg}$ | *HIS3* locus Integration | This Study |
| EZ-L559 | $P_{ADH2}$_GFP_ $T_{ADH1}$ | EMPTY | EMPTY | EMPTY | EMPTY | $HIS3_{Cg}$ | *HIS3* locus Integration | This Study |
| EZ-L561 | $P_{MET3}$_GFP_ $T_{ADH1}$ | EMPTY | EMPTY | EMPTY | EMPTY | $HIS3_{Cg}$ | *HIS3* locus Integration | This Study |
| EZ-L571 | $P_{TEF1}$_ VP16-EL222 _$T_{CYC1}$ | $P_{C120}$_*GAL80*_ $T_{ADH1}$ | EMPTY | $P_{ADH1}$_*GAL4*_ $T_{ACT1}$ | $P_{C120}$_*GAL80*_ $T_{ADH1}$ | $HIS3_{Cg}$ | *HIS3* locus Integration | This Study |

| | | | | | | | | |
|---|---|---|---|---|---|---|---|---|
| EZ-L827 | $P_{C120}$_*PDC*1_T<br>$_{ACT1}$ | $P_{GAL1\text{-}S}$_<br>*LDH*_$T_{ADH1}$ | EMPTY | EMPTY | EMPTY | Zeocin | δ-sites<br>Integration | This<br>Study |
| pMAL81 | $P_{PGK1}$_LexA-<br>hER-B112_<br>$T_{CYC1}$ | $P_{9xLexA_CYC1}$_G<br>FP_$T_{ADH1}$ | EMPTY | EMPTY | EMPTY | $HIS3_{Cg}$ | *HIS3* locus<br>Integration | This<br>Study |
| pMAL125 | $P_{PGK1}$_LexA-<br>hER-VP16_<br>$T_{CYC1}$ | $P_{9xLexA_CYC1}$_G<br>FP_$T_{ADH1}$ | EMPTY | EMPTY | EMPTY | $HIS3_{Cg}$ | *HIS3* locus<br>Integration | This<br>Study |
| pMAL140 | $P_{6xtetO}$_tTA_<br>$T_{ACT1}$ | EMPTY | EMPTY | $P_{7xtetO_CYC1}$_GF<br>P_$T_{ADH1}$ | EMPTY | $HIS3_{Cg}$ | *HIS3* locus<br>Integration | This<br>Study |

MCS = Multiple cloning sites; Gene positions are mapped on the general plasmid structure shown in Supplementary Fig. 12.

Intergenic distances are as previously described.[1]

**Supplementary Table 2. Yeast strains used in study**

| Strain Name | Genotype | Source |
|---|---|---|
| BY4741 | S288C *MAT***a** *his3Δ1 leu2Δ0 met15Δ0 ura3Δ0* | [3] |
| CEN.PK2-1C | *MAT***a** *his3Δ1 leu2*-3_112 *trp1*-289 *ura3*-53 | [4] |
| Y202 | *S288C gal80::KanMX, pdc1Δ, pdc5Δ, pdc6Δ + pJLA121-PDC1$^{0202}$* | [2] |
| YEZ25 | CEN.PK2-1C *gal*80::KanMX | This Study |
| YEZ44 | CEN.PK2-1C *gal*80::KanMX, *gal*4::HygB | [2] |
| YEZ48 | CEN.PK2-1C *HIS3$_{Cg}$*::$P_{GAL1}$_GFP_$T_{ADH1}$ | This Study |
| YEZ94 | Y202 *HIS3$_{Cg}$::$P_{PGK1}$_VP16-EL222 _$T_{CYC1}$* | [2] |
| YEZ100 | YEZ44 *HIS*3$_{Cg}$::($P_{TEF1}$_VP16-EL222 _$T_{CYC1}$, $P_{C120}$_*GAL80*_$T_{ACT1}$, $P_{GAL1}$_GFP_$T_{ADH1}$, $P_{C120}$_*GAL80*_$T_{ADH1}$, $P_{ADH1}$_*GAL4*_$T_{ACT1}$) | [2] |
| YEZ101 | YEZ44 *HIS3$_{Cg}$*::($P_{TEF1}$_VP16-EL222 _$T_{CYC1}$, $P_{C120}$_*GAL80*_$T_{ACT1}$, $P_{GAL1}$_GFP_$T_{ADH1}$, $P_{C120}$_*GAL80*_$T_{ADH1}$, $P_{PGK1}$_*GAL4*_$T_{ACT1}$) | [2] |

| | | |
|---|---|---|
| YEZ102 | YEZ44 *HIS3*$_{Cg}$::($P_{TEF1}$_VP16-EL222 _$T_{CYC1}$, $P_{C120}$_*GAL80*_$T_{ACT1}$, $P_{GAL1}$_GFP_$T_{ADH1}$, $P_{C120}$_*GAL80*_$T_{ADH1}$, $P_{PGK1}$_*GAL4*_PSD_$T_{ACT1}$) | [2] |
| YEZ140 | CEN.PK2-1C *HIS3*$_{cg}$ | [2] |
| YEZ171 | Y202 *HIS3*$_{Cg}$::$P_{TEF1}$_GFP_$T_{CYC1}$ | [2] |
| YEZ186 | CEN.PK2-1C *HIS3*$_{Cg}$::$P_{TEF1}$_GFP_$T_{CYC1}$ | [2] |
| YEZ200 | Y202 *gal80Δ::KanMX, gpd1Δ::*HygB, *pdc1Δ, pdc5Δ, pdc6Δ + pJLA121-PDC1*$^{0202}$ | This Study |
| YEZ203 | YEZ200 *pdc1Δ, pdc5Δ, pdc6Δ gal80Δ gpd1Δ + pJLA121-PDC1*$^{0202}$ | This Study |
| YEZ207 | YEZ203 *HIS3*$_{Cg}$::($P_{TEF1}$_VP16-EL222 _$T_{CYC1}$, $P_{C120}$_*GAL80_ODCmut*_$T_{ACT1}$, $P_{C120}$_*GAL80_ODCmut*_$T_{ADH1}$, $P_{PGK1}$_*GAL4*_PSD_$T_{ACT1}$) | This Study |
| YEZ207C | YEZ203 *HIS3*$_{Cg}$::($P_{TEF1}$_VP16-EL222 _$T_{CYC1}$, $P_{C120}$_*GAL80*_$T_{ACT1}$, $P_{GAL1}$_GFP_$T_{ADH1}$, $P_{C120}$_*GAL80*_$T_{ADH1}$, $P_{PGK1}$_*GAL4*_$T_{ACT1}$) | This Study |
| YEZ209 | Y202 *HIS3*$_{Cg}$::($P_{TEF1}$_VP16-EL222 _$T_{CYC1}$, $P_{C120}$_*GAL80_ODCmut*_$T_{ACT1}$, $P_{GAL1\text{-}S}$_GFP_$T_{ADH1}$, $P_{C120}$_*GAL80_ODCmut*_$T_{ADH1}$, $P_{PGK1}$_*GAL4*_PSD_$T_{ACT1}$) | This Study |

| | | |
|---|---|---|
| YEZ210 | Y202 *HIS3*$_{Cg}$::($P_{TEF1}$_VP16-EL222 _$T_{CYC1}$, $P_{C120}$_*GAL80_ODCmut*_$T_{ACT1}$, $P_{GAL1\text{-}M}$_GFP_$T_{ADH1}$, $P_{C120}$_*GAL80_ODCmut*_$T_{ADH1}$, $P_{PGK1}$_*GAL4*_PSD_$T_{ACT1}$) | This Study |
| YEZ210C | Y202 *HIS3*$_{Cg}$::($P_{TEF1}$_VP16-EL222 _$T_{CYC1}$, $P_{C120}$_*GAL80_ODCmut*_$T_{ACT1}$, $P_{GAL1}$_GFP_$T_{ADH1}$, $P_{C120}$_*GAL80_ODCmut*_$T_{ADH1}$, $P_{PGK1}$_*GAL4*_PSD_$T_{ACT1}$) | This Study |
| YEZ212 | YEZ207 YARCdelta5::($P_{C120}$_*PDC1*_$T_{ACT1}$, $P_{GAL1\text{-}M}$_LDH_$T_{ADH1}$) minus *pJLA121-PDC1*$^{0202}$ | This Study |
| YEZ212C | YEZ207C YARCdelta5::($P_{C120}$_*PDC1*_$T_{ACT1}$, $P_{GAL1\text{-}M}$_LDH_$T_{ADH1}$) minus *pJLA121-PDC1*$^{0202}$ | This Study |
| YEZ228 | CEN.PK2-1C *HIS3*$_{Cg}$::$P_{TDH3}$_GFP_$T_{ADH1}$ | This Study |
| YEZ229 | YEZ25 *HIS3*$_{Cg}$::($P_{TEF1}$_VP16-EL222 _$T_{CYC1}$, $P_{C120}$_*GAL80_ODCmut*_$T_{ACT1}$, $P_{GAL1\text{-}S}$_GFP_$T_{ADH1}$, $P_{C120}$_*GAL80_ODCmut*_$T_{ADH1}$, $P_{PGK1}$_*GAL4*_PSD_$T_{ACT1}$) | This Study |
| YEZ230 | YEZ25 *HIS3*$_{Cg}$::($P_{TEF1}$_VP16-EL222 _$T_{CYC1}$, $P_{C120}$_*GAL80_ODCmut*_$T_{ACT1}$, $P_{GAL1\text{-}M}$_GFP_$T_{ADH1}$, $P_{C120}$_*GAL80_ODCmut*_$T_{ADH1}$, $P_{PGK1}$_*GAL4*_PSD_$T_{ACT1}$) | This Study |
| YEZ230-5 | YEZ25 *HIS3*$_{Cg}$::($P_{TEF1}$_VP16-EL222 _$T_{CYC1}$, $P_{C120}$_*GAL80_CLN2PEST*_$T_{ACT1}$, $P_{GAL1}$_GFP_$T_{ADH1}$, $P_{C120}$_*GAL80_CLN2PEST*_$T_{ACT1}$, $P_{PGK1}$_*GAL4*_PSD_$T_{ADH1}$) | This Study |

| | | |
|---|---|---|
| YEZ230C | YEZ25 *HIS3*$_{Cg}$::($P_{TEF1}$_VP16-EL222 _$T_{CYC1}$, $P_{C120}$_*GAL80_ODCmut*_$T_{ACT1}$, $P_{GAL1}$_GFP_$T_{ADH1}$, $P_{C120}$_*GAL80_ODCmut*_$T_{ADH1}$, $P_{PGK1}$_*GAL4*_PSD_$T_{ACT1}$) | This Study |
| YEZ235 | CEN.PK2-1C *gpd1Δ*::HygB, *pdc1Δ, pdc5Δ, pdc6Δ gal80Δ ald6Δ bat1Δ + pJLA121-PDC1*$^{0202}$ | This Study |
| YEZ294 | CEN.PK2-1C *HIS3*$_{Cg}$::$P_{ADH2}$_GFP_$T_{ADH1}$ | This Study |
| YEZ295 | CEN.PK2-1C *HIS3*$_{Cg}$::$P_{MET31}$_GFP_$T_{ADH1}$ | This Study |
| YEZ531 | YEZ235 *HIS3*$_{Cg}$::($P_{TEF1}$_VP16-EL222_$T_{CYC1}$, $P_{C120}$_*GAL80*_$T_{ADH1}$, $P_{ADH1}$_*GAL4*_$T_{ACT1}$, $P_{C120}$_*GAL80*_$T_{ADH1}$) | This Study |
| YEZ532 | YEZ235 *HIS3*$_{Cg}$::($P_{TEF1}$_VP16-EL222_$T_{CYC1}$, $P_{C120}$_*GAL80_ODCmut*_$T_{ACT1}$, $P_{C120}$_*GAL80_ODCmut*_$T_{ADH1}$, $P_{PGK1}$_*GAL4*_PSD_$T_{ACT}$) | This Study |
| YEZ535 | YEZ531 YARCdelta5::($P_{C120}$_*PDC1*_$T_{ACT1}$,-$P_{GAL1-M}$_ILV2_$T_{ADH1}$) minus *pJLA121-PDC1*$^{0202}$ | This Study |
| YEZ536 | YEZ532 YARCdelta5::($P_{C120}$_*PDC1*_$T_{ACT1}$,-$P_{GAL1-M}$_ILV2_$T_{ADH1}$) minus *pJLA121-PDC1*$^{0202}$ | This Study |

| | | |
|---|---|---|
| YEZ544-1 | YEZ535 + EZ-L390 | This Study |
| YEZ546-2 | YEZ536 + EZ-L390 | This Study |
| YEZ597-5 | YEZ207C YARCdelta5::($P_{C120}$_*PDC1*_$T_{ACT1}$, $P_{GAL1-S}$_LDH_$T_{ADH1}$) minus *pJLA121-PDC1*$^{0202}$ | This Study |
| YEZ598-4 | YEZ207 YARCdelta5::($P_{C120}$_*PDC1*_$T_{ACT1}$, $P_{GAL1-S}$_LDH_$T_{ADH1}$) minus *pJLA121-PDC1*$^{0202}$ | This Study |
| YEZ636 | CEN.PK2-1C *HIS3*$_{Cg}$:: $P_{GAL1-S}$_GFP_$T_{ADH1}$ | This Study |
| yMAL34 | CEN.PK2-1C *HIS3*$_{Cg}$::$P_{PGK1}$_LexA-hER-B112_$T_{CYC1}$, $P_{9xLexA_CYC1}$_GFP_$T_{ADH1}$ | This Study |
| yMAL35 | CEN.PK2-1C *HIS3*$_{Cg}$::$P_{PGK1}$_LexA-hER-VP16_$T_{CYC1}$, $P_{9xLexA_CYC1}$_GFP_$T_{ADH1}$ | This Study |
| yMAL36 | CEN.PK2-1C *HIS3*$_{Cg}$::$P_{6xtetO}$_tTA_$T_{ACT1}$, $P_{7xtetO_CYC1}$_GFP_$T_{ADH1}$ | This Study |

**Supplementary Figures:**

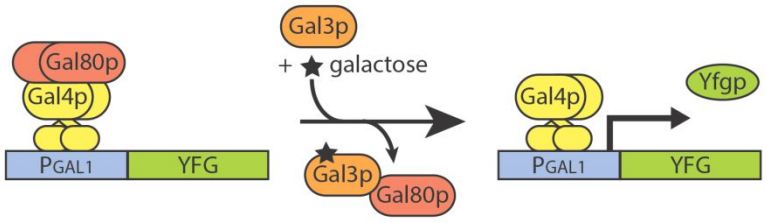


**Supplementary Figure 1. The endogenous galactose regulation system**

In carbon sources other than galactose, Gal80p represses Gal4p activation of genes controlled by $P_{GAL1}$. When the cells are grown in galactose, Gal3p is allosterically activated by galactose and binds to Gal80p to carry it out of the nucleus. Gal4p is also more highly expressed in galactose media.

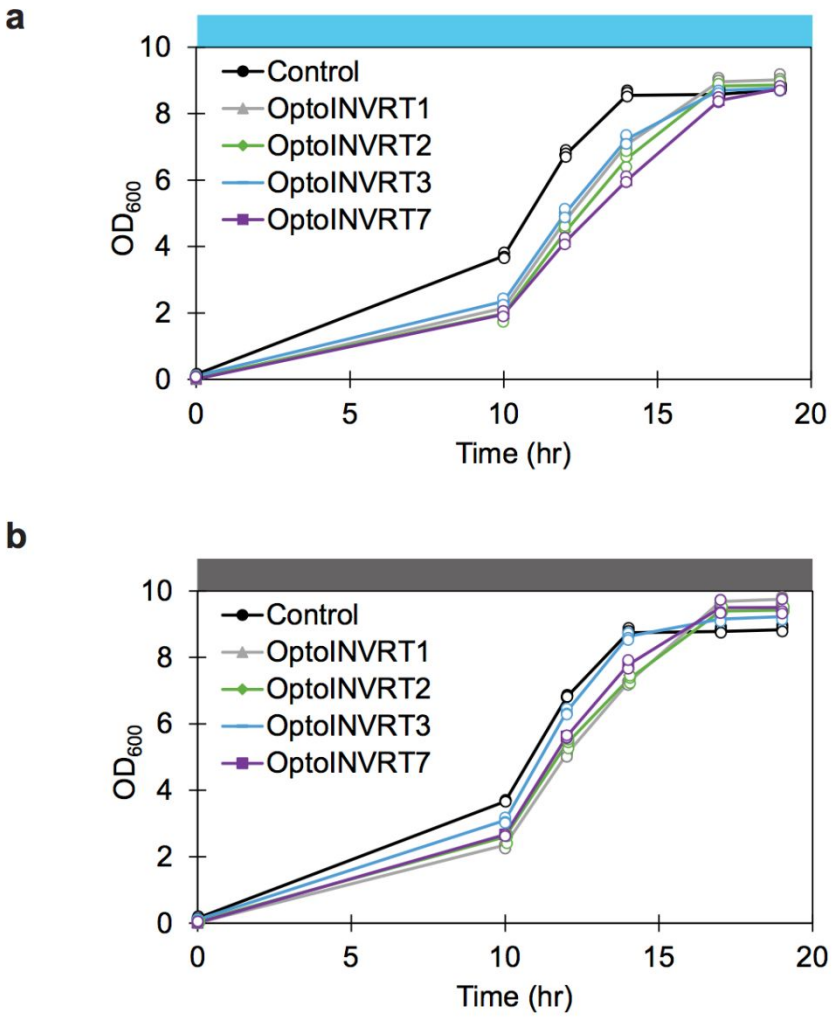


**Supplementary Figure 2. Impact of OptoINVRT circuits on cell growth.**

Growth curves of cells containing OptoINVRT1 (YEZ100), OptoINVRT2 (YEZ101), OptoINVRT3 (YEZ102), and OptoINVRT7 (YEZ230C), compared to a wild type control (YEZ140) in full blue light (**a**) and dark (**b**) conditions. Data points of three independent replicates are shown.

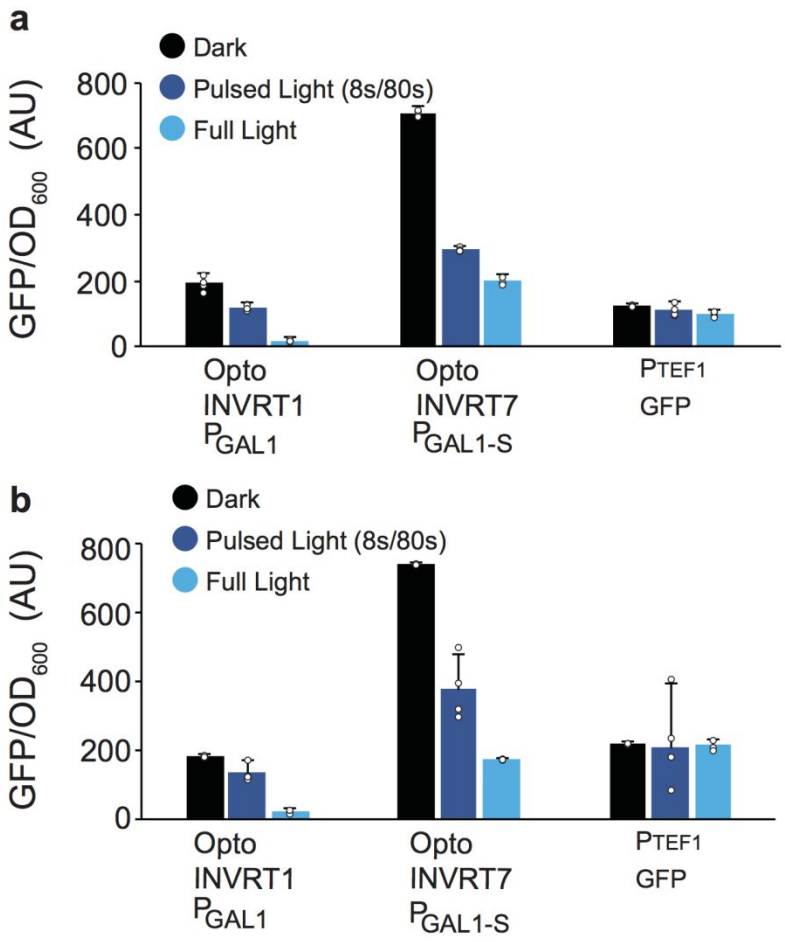


**Supplementary Figure 3. Activity of OptoINVRT circuits and $P_{GAL1-S}$ in different carbon sources**

Activity of OptoINVRT1-$P_{GAL1}$ (YEZ100) and OptoINVRT7-$P_{GAL1-S}$ (YEZ229) in 2% ethanol **(a)** or 2% glycerol **(b)** as sole carbon sources. For all experiments, a positive control strain expressing GFP under $P_{TEF1}$ (YEZ186) was included in each repeat, and YEZ140 (no GFP control) was used to subtract background and auto-fluorescence. All data are shown as mean values; dots represent individual data points; error bars represent the s.d. of four biologically independent 1-ml sample replicates exposed to the same conditions. All experiments were repeated at least three times.

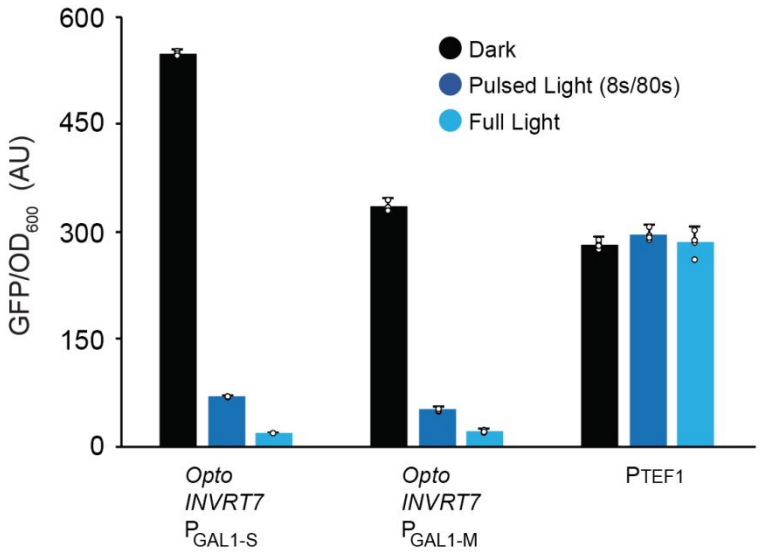


**Supplementary Figure 4. Activity of OptoINVRT7 and $P_{GAL1}$ engineered promoters in a yeast S288C (BY4741) background strain (Y202)**

Specific expression of GFP using OptoINVRT7 with $P_{GAL1-S}$ (YEZ209) or $P_{GAL1-M}$ (YEZ210) in an S288C background strain (Y202; S288C, *pdc1*Δ, *pdc5*Δ, *pdc6*Δ, *gal80Δ* containing pJLA121PDC1$^{0202}$), compared to constitutive expression using $P_{TEF1}$ (YEZ171) in the same background. This background is used for lactic acid and isobutanol production. YEZ94 (no GFP control) was used to subtract background and auto-fluorescence. All data are shown as mean values; dots represent individual data points; error bars represent the s.d. of four biologically independent 1-ml sample replicates exposed to the same conditions. All experiments were repeated at least three times.

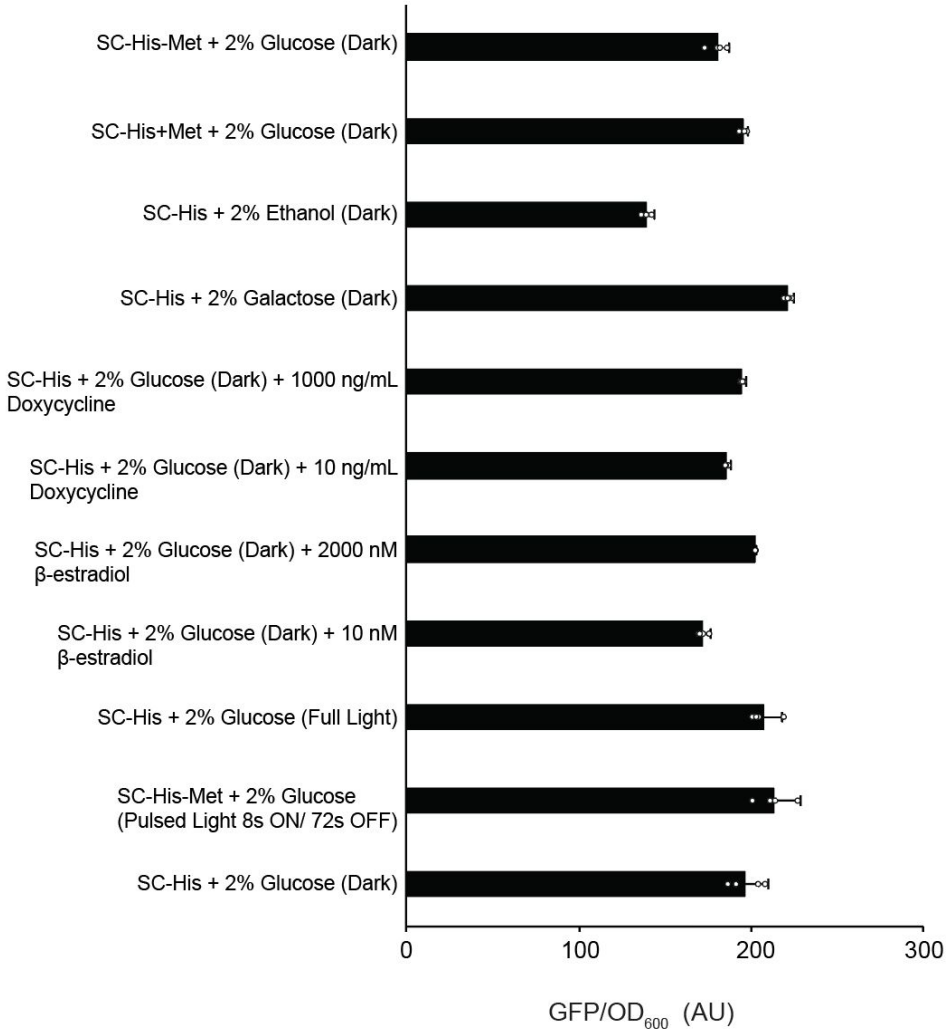


**Supplementary Figure 5. GFP expression using $P_{TEF1}$ in different conditions**

Specific expression of GFP using $P_{TEF1}$ in different media and light conditions, used as controls for experiments shown in Figure 1d. YEZ186 ($P_{TEF1}$-GFP) was grown in different media and light conditions. YEZ140 (no GFP control) was used to subtract background and auto-fluorescence. All data are shown as mean values; dots represent individual data points; error bars represent the s.d. of four biologically independent 1-ml sample replicates exposed to the same conditions. All experiments were repeated at least three times.

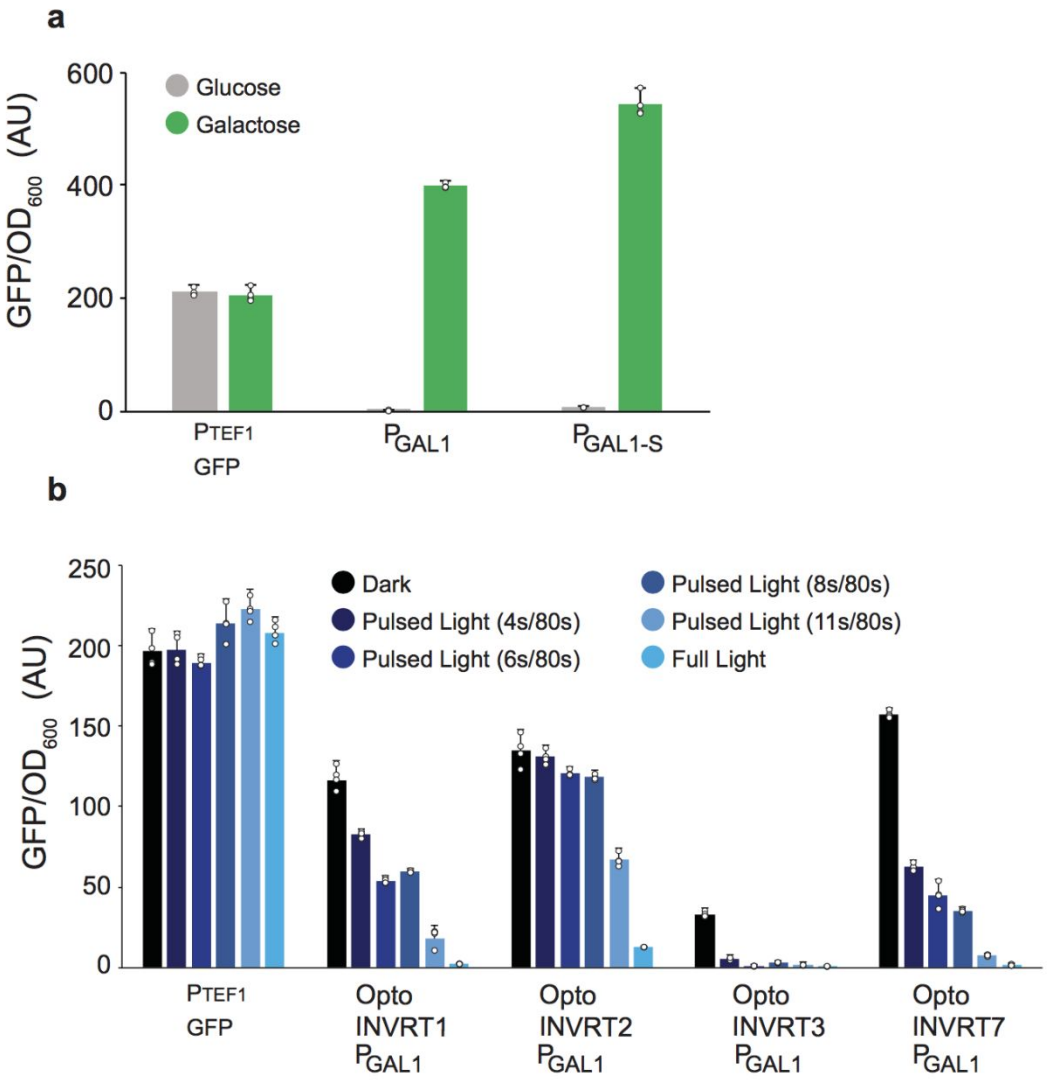


**Supplementary Figure 6. Activation of $P_{GAL1-S}$ in galactose and light-tunability of OptoINVRT Circuits**

**(a)** Light-independent activation of $P_{GAL1-S}$ by galactose: strains expressing GFP under $P_{GAL1}$ (YEZ48) or $P_{GAL1-S}$ (YEZ636), without any optogenetic circuit, grown in either 2% glucose or 2% galactose as sole carbon sources. **(b)** Response of different OptoINVRT circuits to different duty cycles of light. Circuits were compared in CENPK.2-1C-derived (*gal80Δ, gal4Δ* for OptoINVRT1,2,3; *gal80Δ* for OptoINVRT5,7) strains: YEZ100 (OptoINVRT1), YEZ101

(OptoINVRT2), YEZ102 (OptoINVRT3), YEZ230-5 (OptoINVRT5) and YEZ230C (OptoINVRT7). Specific expression of GFP under constitutive $P_{TEF1}$ (YEZ186) is shown as control. YEZ140 (no GFP control) was used to subtract background and auto-fluorescence. All data are shown as mean values; dots represent individual data points; error bars represent the s.d. of four biologically independent 1-ml sample replicates exposed to the same conditions. All experiments were repeated at least three times.

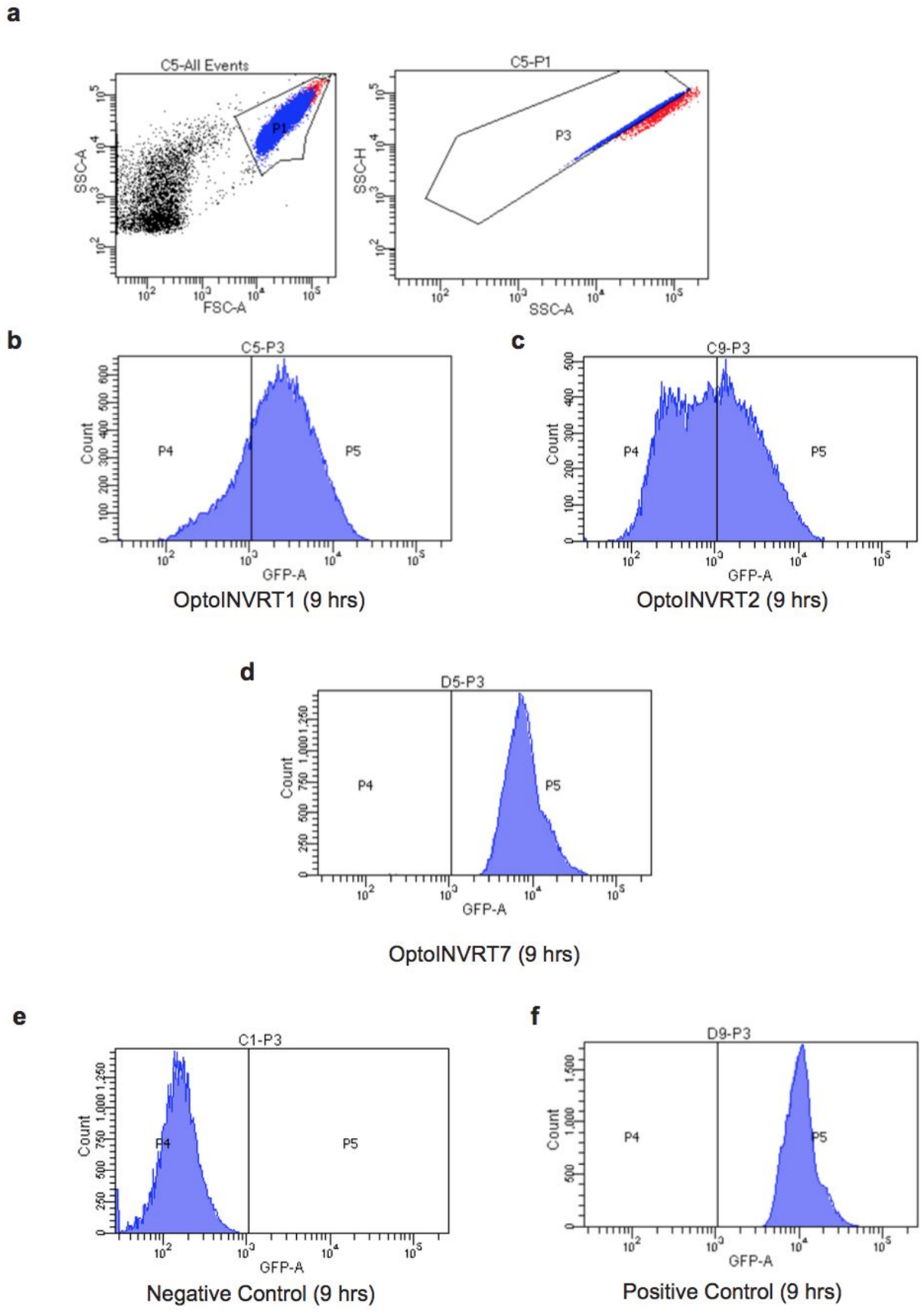
a
C5-All Events
P1
SSC-A
FSC-A
C5-P1
P3
SSC-H
SSC-A
b
C5-P3
P4
P5
Count
GFP-A
OptoINVRT1 (9 hrs)
c
C9-P3
P4
P5
Count
GFP-A
OptoINVRT2 (9 hrs)
d
D5-P3
P4
P5
Count
GFP-A
OptoINVRT7 (9 hrs)
e
C1-P3
P4
P5
Count
GFP-A
Negative Control (9 hrs)
f
D9-P3
P4
P5
Count
GFP-A
Positive Control (9 hrs)

**Supplementary Figure 7. Flow cytometry histograms**

**(a)** The FSC vs. SSC plot shows the gating for isolating yeast cell events (left panel), while the SSC-H vs. SSC-A plot shows the gating for isolating single cell events (right panel). **(b-f)** Representative histograms of GFP expression for OptoINVRT1 **(b)**, OptoINVRT2 **(c)**, OptoINVRT7 **(d)**, negative control **(e)**, and positive control **(f)** measured 9 hours after induction of gene expression, corresponding to the data shown in Figure 3.

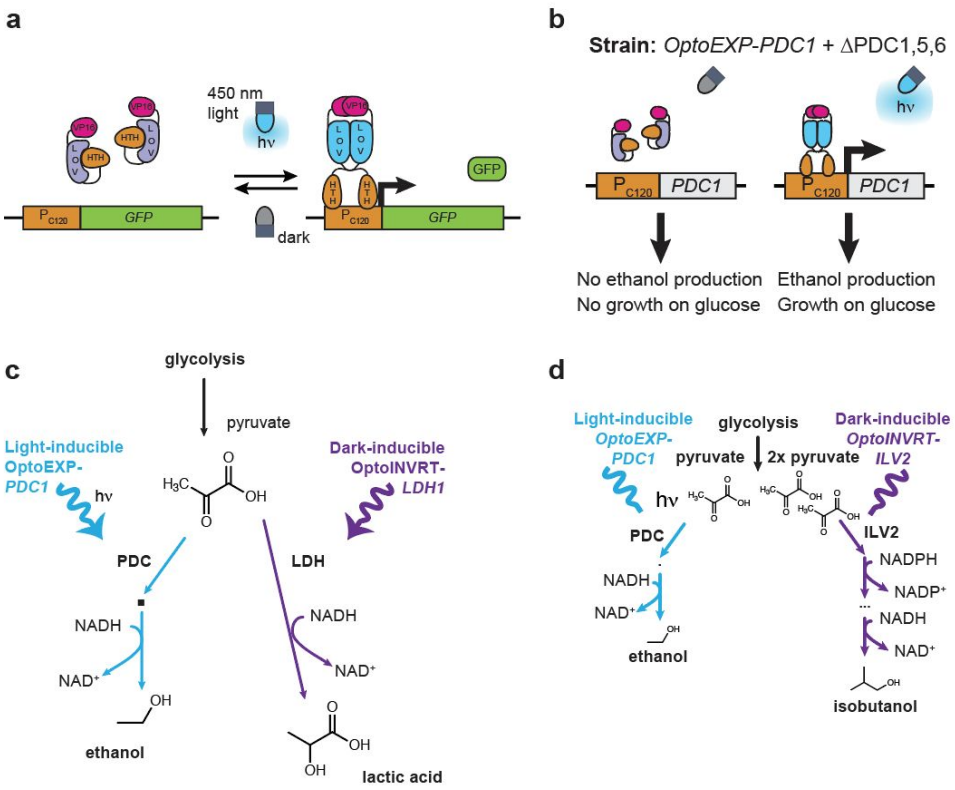


**Supplementary Figure 8. Schematics for OptoEXP and biosynthetic pathways**

**(a)** Mechanism of OptoEXP, where light-responsive VP16-EL222 activates gene expression[2]. **(b)** OptoEXP control of *PDC1* in our triple *PDC* deletion strains used for lactic acid and isobutanol production[2]. **(c)** Lactic acid biosynthetic pathway, where *PDC1* is control with OptoEXP, and LDH with OptoINVRT circuits[2]. **(d)** Isobutanol biosynthetic pathway, where *PDC1* is controlled with OptoEXP and *ILV2* with OptoINVRT circuits.[2]

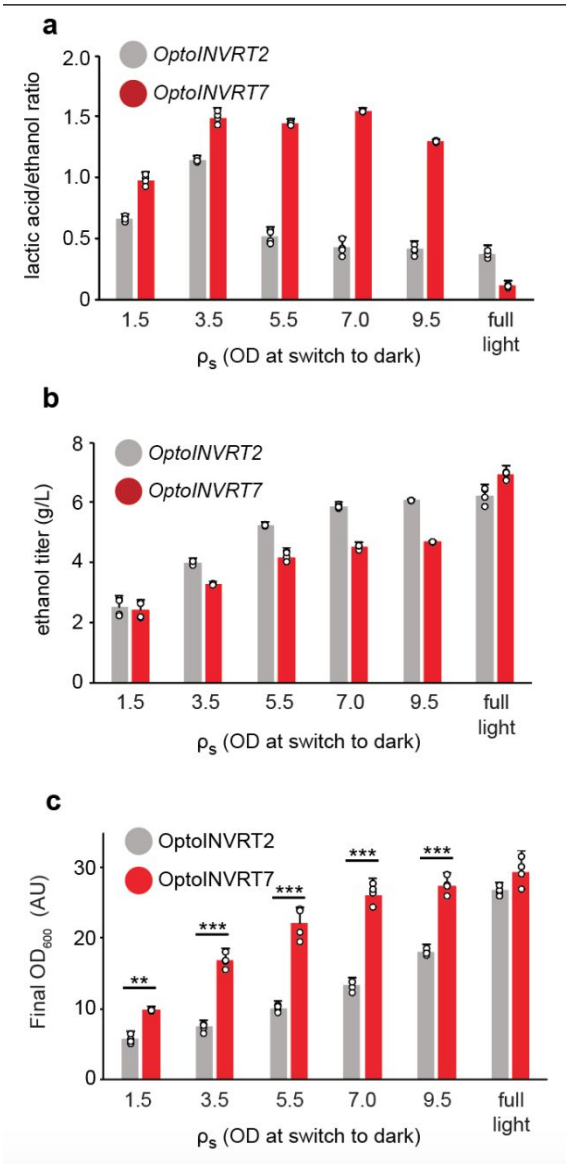


**Supplementary Figure 9. Ethanol production and cell growth during LA fermentations**

The ratio of lactic acid to ethanol titers **(a),** ethanol titers **(b)**, and final cell density after 48-hour fermentations **(c)**, measured at different $\rho_s$ values, and using OptoINVRT2 (YEZ212C, gray) or OptoINVRT7 (YEZ212, red). All data are shown as mean values; dots represent individual data points; error bars represent the s.d. of four biologically independent 1-ml sample replicates exposed to the same conditions. All experiments were repeated at least three times.

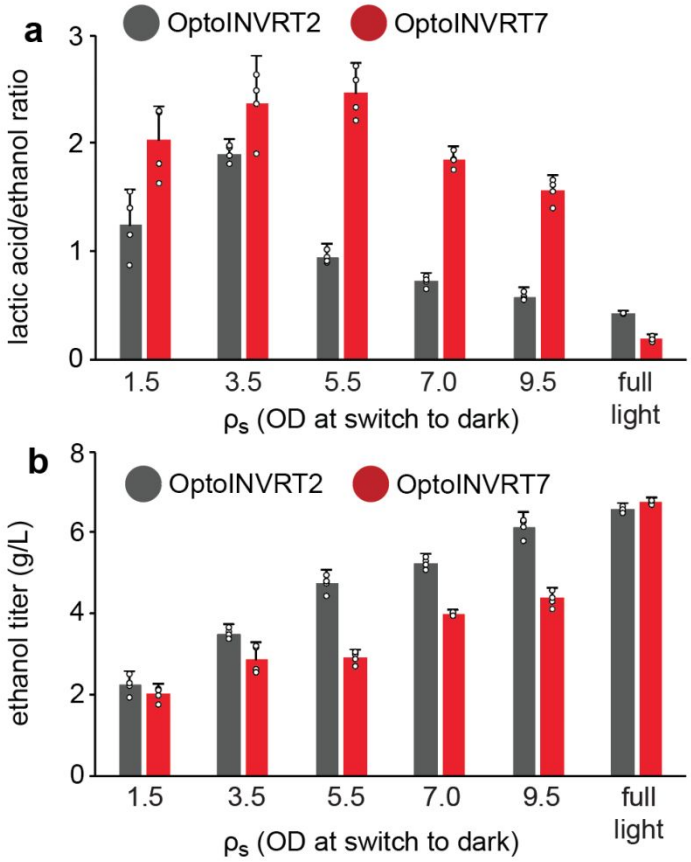


**Supplementary Figure 10. Ethanol production by OptoINVRT circuits regulating $P_{GAL1\text{-}S}$**

Lactic acid to ethanol titer ratios **(a)** and ethanol titers **(b),** at different $\rho_s$, of strains using $P_{GAL1\text{-}S}$ to express LDH, controlled by OptoINVRT2 (gray, YEZ597-5) or OptoINVRT7 (red, YEZ598-4). All data are shown as mean values; dots represent individual data points; error bars represent the s.d. of four biologically independent 1-ml sample replicates exposed to the same conditions. All experiments were repeated at least three times.

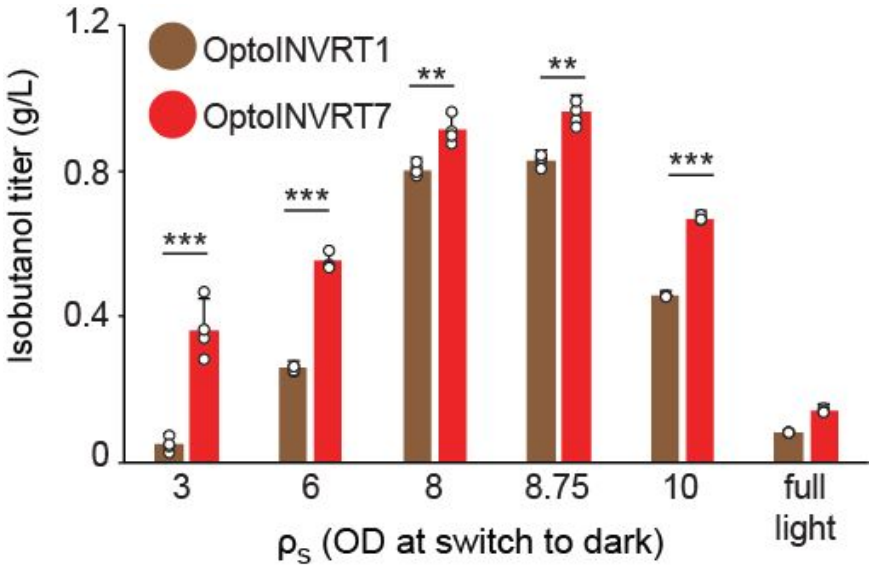


**Supplementary Figure 11. Comparison of optogenetic circuits for lactic acid and isobutanol production.** Isobutanol production at different $\rho_s$ values using OptoINVRT1 (YEZ544-1) and OptoINVRT7 (YEZ546-2) with $P_{GAL1\text{-}M}$; full light samples were kept under continuous light throughout growth and production phases. $^{**}P < 0.01$, $^{***}P < 0.001$. Statistics are derived using a one-sided *t*-test. All data are shown as mean values; dots represent individual data points; error bars represent the s.d. of four biologically independent 1-ml sample replicates exposed to the same conditions. All experiments were repeated at least three times.

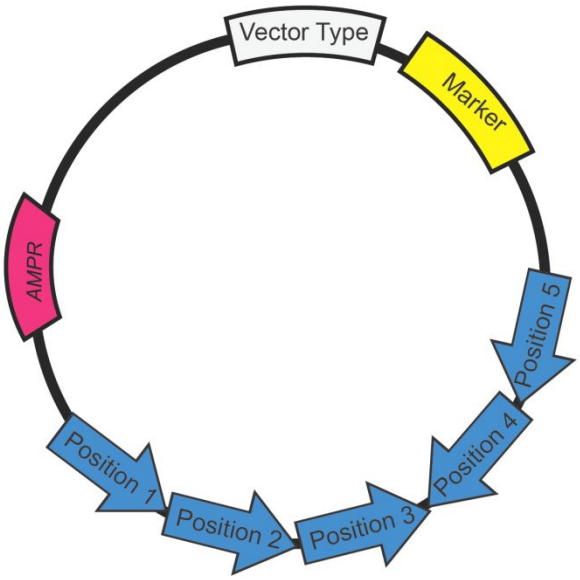


225

226 **Supplementary Figure 12. General scheme of vectors**

227 General vector map showing the relative orientation of the five positions listed in Supplementary
228 Table 1. Different genes (including promoters and terminators) were assembled using a
229 previously described multiple gene insertion strategy[1]. All vectors have an ampicillin resistance
230 marker (*AMPR*) for cloning in *E. coli* and a selection marker for *S. cerevisiae* (Marker). Vector
231 types include 2μ, or integrative[5–7].

232

233

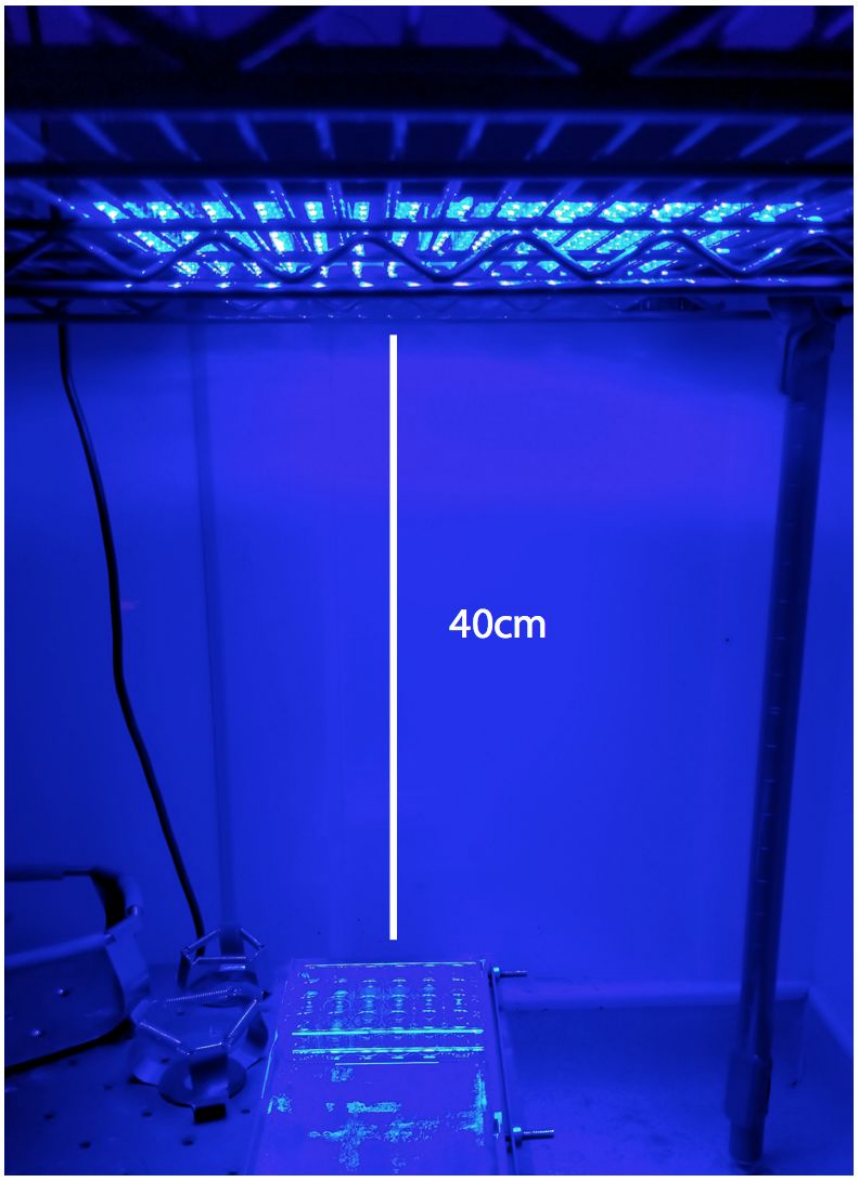


**Supplementary Figure 13. Light panel setup**

Picture of experimental setup for protocols involving light stimulation. Light panels were placed 40 cm above 24-well plates, which were shaken at 200 RPM in a warm room (set to 30°C) with ambient lights turned off.

## Supplementary References


1. Avalos, J. L., Fink, G. R. & Stephanopoulos, G. Compartmentalization of metabolic pathways in yeast mitochondria improves the production of branched-chain alcohols. *Nat. Biotechnol.* **31**, 335–341 (2013).
2. Zhao, E. M. *et al.* Optogenetic regulation of engineered cellular metabolism for microbial chemical production. *Nature* **555**, 683–687 (2018).
3. Brachmann, C. B. *et al.* Designer deletion strains derived from Saccharomyces cerevisiae S288C: A useful set of strains and plasmids for PCR-mediated gene disruption and other applications. *Yeast* **14**, 115–132 (1998).
4. Entian, K. D. & Kötter, P. 25 Yeast Genetic Strain and Plasmid Collections. *Methods in Microbiology* vol. 36 629–666 (2007).
5. Chee, M. K. & Haase, S. B. New and Redesigned pRS Plasmid Shuttle Vectors for Genetic Manipulation of Saccharomyces cerevisiae. *Genes|Genomes|Genetics* **2**, 515–526 (2012).
6. Yuan, J. & Ching, C. B. Combinatorial Assembly of Large Biochemical Pathways into Yeast Chromosomes for Improved Production of Value-added Compounds. *ACS Synth. Biol.* **4**, 23–31 (2014).
7. Goldstein, A. L. & McCusker, J. H. Three new dominant drug resistance cassettes for gene disruption in Saccharomyces cerevisiae. *Yeast* **15**, 1541–1553 (1999).